

---

# Deep $k$ -Means: Jointly Clustering with $k$ -Means and Learning Representations

---

**Maziar Moradi Fard**

Univ. Grenoble Alpes, CNRS, Grenoble INP – LIG  
maziar.moradi-fard@univ-grenoble-alpes.fr

**Thibaut Thonet**

Univ. Grenoble Alpes, CNRS, Grenoble INP – LIG  
thibaut.thonet@univ-grenoble-alpes.fr

**Eric Gaussier**

Univ. Grenoble Alpes, CNRS, Grenoble INP – LIG, Skopai  
eric.gaussier@univ-grenoble-alpes.fr

## Abstract

We study in this paper the problem of jointly clustering and learning representations. As several previous studies have shown, learning representations that are both faithful to the data to be clustered and adapted to the clustering algorithm can lead to better clustering performance, all the more so that the two tasks are performed jointly. We propose here such an approach for  $k$ -Means clustering based on a continuous reparametrization of the objective function that leads to a truly joint solution. The behavior of our approach is illustrated on various datasets showing its efficacy in learning representations for objects while clustering them.

## 1 Introduction

Clustering is a long-standing problem in the machine learning and data mining fields, and thus accordingly fostered abundant research. Traditional clustering methods, *e.g.*,  $k$ -Means [21] and Gaussian Mixture Models (GMMs) [5], fully rely on the original data representations and may then be ineffective when the data points (*e.g.*, images and text documents) live in a high-dimensional space – a problem commonly known as the curse of dimensionality. Significant progress has been made in the last decade or so to learn better, low-dimensional data representations [12]. The most successful techniques to achieve such high-quality representations rely on deep neural networks (DNNs), which apply successive non-linear transformations to the data in order to obtain increasingly high-level features. Auto-encoders (AEs) are a special instance of DNNs which are trained to embed the data into a (usually dense and low-dimensional) vector at the bottleneck of the network, and then attempt to reconstruct the input based on this vector. The appeal of AEs lies in the fact that they are able to learn representations in a fully unsupervised way. The representation learning breakthrough enabled by DNNs spurred the recent development of numerous deep clustering approaches which aim at jointly learning the data points’ representations as well as their cluster assignments.

In this study, we specifically focus on the  $k$ -Means-related deep clustering problem. Contrary to previous approaches that alternate between continuous gradient updates and discrete cluster assignment steps [30], we show here that one can solely rely on gradient updates to learn, truly jointly, representations and clustering parameters. This ultimately leads to a better deep  $k$ -Means method which is also more scalable as it can fully benefit from the efficiency of stochastic gradient

descent (SGD). In addition, we perform a careful comparison of different methods by (a) relying on the same auto-encoders, as the choice of auto-encoders impacts the results obtained, (b) tuning the hyperparameters of each method on a small validation set, instead of setting them without clear criteria, and (c) enforcing, whenever possible, that the same initialization and sequence of SGD minibatches are used by the different methods. The last point is crucial to compare different methods as these two factors play an important role and the variance of each method is usually not negligible.

The remainder of the study is organized as follows: Section 2 presents the related work; Section 3 describes the approach we propose whereas Section 4 presents the empirical validation of this approach on various datasets. Lastly, Section 5 concludes the paper.

## 2 Related work

In the wake of the groundbreaking results obtained by DNNs in computer vision, several deep clustering algorithms were specifically designed for image clustering [31, 7, 9, 14, 13]. These works have in common the exploitation of Convolutional Neural Networks (CNNs), which extensively contributed to last decade’s significant advances in computer vision. Inspired by agglomerative clustering, [31] proposed a recurrent process which successively merges clusters and learn image representations based on CNNs. In [7], the clustering problem is formulated as binary pairwise-classification so as to identify the pairs of images which should belong to the same cluster. Due to the unsupervised nature of clustering, the CNN-based classifier in this approach is only trained on noisily labeled examples obtained by selecting increasingly difficult samples in a curriculum learning fashion. [9] jointly trained a CNN auto-encoder and a multinomial logistic regression model applied to the AE’s latent space. Similarly, [13] alternates between representation learning and clustering where mini-batch  $k$ -Means is utilized as the clustering component. Differently from these works, [14] proposed an information-theoretic framework based on data augmentation to learn discrete representations, which may be applied to clustering or hash learning. Although these different algorithms obtained state-of-the-art results on image clustering [1], their ability to generalize to other types of data (e.g., text documents) is not guaranteed due to their reliance on essentially image-specific techniques – Convolutional Neural Network architectures and data augmentation.

Nonetheless, many general-purpose – non-image-specific – approaches to deep clustering have also been recently designed [15, 25, 29, 8, 11, 14, 17, 18, 24, 30]. Generative models were proposed in [8, 18] which combine variational AEs and GMMs to perform clustering. Alternatively, [25, 24, 17] framed deep clustering as a subspace clustering problem in which the mapping from the original data space to a low-dimensional subspace is learned by a DNN.

Few approaches were directly influenced by  $k$ -Means clustering [15, 29, 11, 30]. The Deep Embedding Network (DEN) model [15] first learns representations from an AE while enforcing locality-preserving constraints and group sparsity; clusters are then obtained by simply applying  $k$ -Means to these representations. Yet, as representation learning is decoupled from clustering, the performance is not as good as the one obtained by methods that rely on a joint approach. [29] defined the Deep Embedded Clustering (DEC) method which simultaneously updates the data points’ representations, initialized from a pre-trained AE, and cluster centers. However, instead of relying on hard cluster assignments as in  $k$ -Means, DEC opted for soft assignments which are optimized to match stricter assignments through a Kullback-Leibler divergence loss. IDEC was subsequently proposed in [11] as an improvement to DEC by integrating the AE’s reconstruction error in the objective function.

Besides [13], mentioned before in the context of images, the only study, to our knowledge, that directly addresses the problem of jointly learning representations and clustering with  $k$ -Means (and not an approximation of it) is the Deep Clustering Network (DCN) approach [30]. However, as in [13], DCN alternatively learns (rather than jointly learns) the object representations, the cluster centroids and the cluster assignments, the latter being based on discrete optimization steps which cannot benefit from the efficiency of stochastic gradient descent. The approach proposed here, entitled *Deep  $k$ -Means* (DKM), addresses this problem.

## 3 Deep $k$ -Means

In the remainder,  $x$  denotes an object from a set  $\mathcal{X}$  of objects to be clustered.  $\mathbb{R}^p$  represents the space in which learned data representations are to be embedded.  $K$  is the number of clusters to

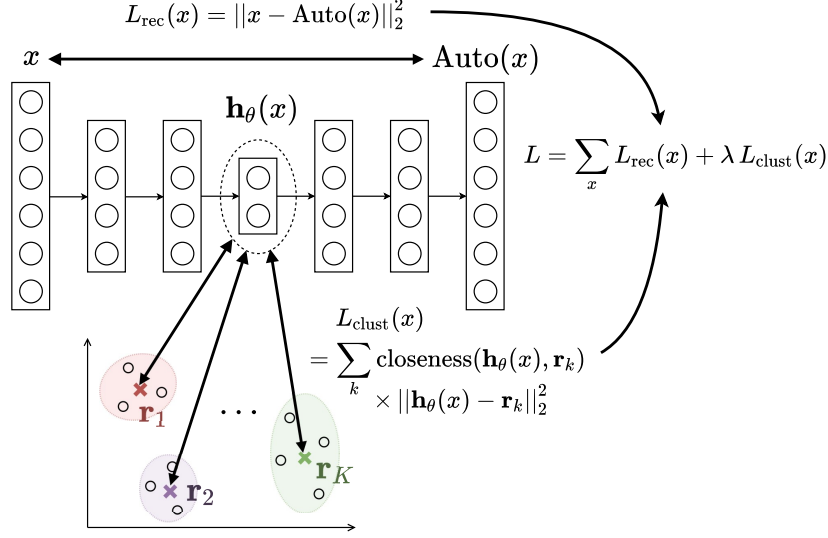


Figure 1: Overview of the proposed Deep k-Means approach instantiated with losses based on the Euclidean distance.

be obtained,  $\mathbf{r}_k \in \mathbb{R}^p$  the representative of cluster  $k$ ,  $1 \leq k \leq K$ , and  $\mathcal{R} = \{\mathbf{r}_1, \dots, \mathbf{r}_K\}$  the set of representatives. Functions  $f$  and  $g$  define some distance or similarity in  $\mathbb{R}^p$  which are assumed to be fully differentiable wrt their variables. For any vector  $\mathbf{y} \in \mathbb{R}^p$ ,  $c_f(\mathbf{y}; \mathcal{R})$  gives the closest representative of  $\mathbf{y}$  according to  $f$ .

Introducing two sign variables,  $\epsilon_0$  and  $\epsilon_1$ , the deep  $k$ -Means problem takes the form:

$$\begin{aligned} \min_{\mathcal{R}, \theta} \sum_{x \in \mathcal{X}} \epsilon_0 g(x, A(x; \theta)) + \lambda \epsilon_1 f(\mathbf{h}_\theta(x), c_f(\mathbf{h}_\theta(x); \mathcal{R})), \\ \text{with: } c_f(\mathbf{h}_\theta(x); \mathcal{R}) = \underset{\mathbf{r} \in \mathcal{R}}{\operatorname{argmin}} \epsilon_1 f(\mathbf{h}_\theta(x), \mathbf{r}) \end{aligned} \quad (1)$$

$g$  measures the error between an object  $x$  and its reconstruction  $A(x; \theta)$  provided by an auto-encoder,  $\theta$  representing the set of the auto-encoder's parameters. A regularization term on  $\theta$  can be included in the definition of  $g$ . However, as most auto-encoders do not use regularization, we dispense with such a term here.  $\mathbf{h}_\theta(x)$  denotes the representation of  $x$  in  $\mathbb{R}^p$  output by the AE's encoder part and  $f(\mathbf{h}_\theta(x), c_f(\mathbf{h}_\theta(x); \mathcal{R}))$  is the clustering loss corresponding to the  $k$ -Means objective function in the embedding space. Finally,  $\lambda$  in Problem (1) regulates the trade-off between seeking good representations for  $x$  – *i.e.*, representations that are faithful to the original examples – and representations that are useful for clustering purposes.

The sign variables  $\epsilon_0$  and  $\epsilon_1$  are set as follows:

$$\epsilon_0 \text{ (resp. } \epsilon_1) = \begin{cases} +1 & \text{if } g \text{ (resp. } f) \text{ is a distance,} \\ -1 & \text{if } g \text{ (resp. } f) \text{ is a similarity function.} \end{cases}$$

Figure 1 illustrates the overall framework retained in this study with  $f$  and  $g$  both based on the Euclidean distance. The closeness term in the clustering loss will be further clarified below.

We now introduce a parameterized version of the above problem that constitutes a *continuous generalization*, whereby we mean here that all functions considered are continuous wrt the introduced parameter. To do so, we first note that the clustering objective function can be rewritten as  $f(\mathbf{h}_\theta(x), c_f(\mathbf{h}_\theta(x); \mathcal{R})) = \sum_{k=1}^K f_k(\mathbf{h}_\theta(x); \mathcal{R})$  with:

$$f_k(\mathbf{h}_\theta(x); \mathcal{R}) = \begin{cases} f(\mathbf{h}_\theta(x), \mathbf{r}_k) & \text{if } \mathbf{r}_k = c_f(\mathbf{h}_\theta(x); \mathcal{R}) \\ 0 & \text{otherwise} \end{cases}$$

Let us now assume that we know some function  $G_{k,f}(\mathbf{h}_\theta(x), \alpha; \mathcal{R})$  such that:

- (i)  $G_{k,f}$  is differentiable wrt to  $\theta, \mathcal{R}$  and continuous wrt  $\alpha$  (differentiability wrt  $\mathcal{R}$  means differentiability wrt to all dimensions of  $\mathbf{r}_k$ ,  $1 \leq k \leq K$ );
- (ii)  $\exists \alpha_0 \in \mathbb{R} \cup \{-\infty, +\infty\}$  such that:

$$\lim_{\alpha \rightarrow \alpha_0} G_{k,f}(\mathbf{h}_\theta(x), \alpha; \mathcal{R}) = \begin{cases} 1 & \text{if } \mathbf{r}_k = c_f(\mathbf{h}_\theta(x); \mathcal{R}) \\ 0 & \text{otherwise} \end{cases}$$

Then, one has:

**Lemma 3.1**  $\forall x \in \mathcal{X}$ :

$$\lim_{\alpha \rightarrow \alpha_0} f(\mathbf{h}_\theta(x), \mathbf{r}_k) G_{k,f}(\mathbf{h}_\theta(x), \alpha; \mathcal{R}) = f_k(\mathbf{h}_\theta(x); \mathcal{R})$$

The proof directly derives from the definitions of  $f_k$  and  $G_{k,f}$ .

From Lemma 3.1, one can see that:

**Property 3.1** *The problem given in (1) is equivalent to:*

$$\min_{\mathcal{R}, \theta} \lim_{\alpha \rightarrow \alpha_0} \sum_{x \in \mathcal{X}} \epsilon_0 g(x, A(x; \theta)) + \lambda \epsilon_1 \overbrace{\sum_{k=1}^K f(\mathbf{h}_\theta(x), \mathbf{r}_k) G_{k,f}(\mathbf{h}_\theta(x), \alpha; \mathcal{R})}^{\mathcal{F}(\mathcal{X}, \alpha; \theta, \mathcal{R})} \quad (2)$$

All functions in the above formulation are fully differentiable wrt both  $\theta$  and  $\mathcal{R}$ . One can thus estimate  $\theta$  and  $\mathcal{R}$  through a simple, joint optimization based on stochastic gradient descent (SGD) for a given  $\alpha$ :

$$(\theta, \mathcal{R}) \leftarrow (\theta, \mathcal{R}) - \eta \frac{1}{|\tilde{\mathcal{X}}|} \nabla_{(\theta, \mathcal{R})} \mathcal{F}(\tilde{\mathcal{X}}, \alpha; \theta, \mathcal{R}) \quad (3)$$

with  $\eta$  the learning rate and  $\tilde{\mathcal{X}}$  a random mini-batch of  $\mathcal{X}$ .

### 3.1 Choice of $G_{k,f}$

Several choices are possible for  $G_{k,f}$ . A simple choice, used throughout this study, is based on a parameterized softmax function. The fact that the softmax function can be used as a differentiable surrogate to argmax or argmin is well known and has been applied in different contexts, as in the recently proposed Gumbel-softmax distribution employed to approximate categorical samples [16, 22]. The parameterized softmax function which we adopted takes the following form:

$$G_{k,f}(\mathbf{h}_\theta(x), \alpha; \mathcal{R}) = \frac{e^{-\epsilon_1 \alpha f(\mathbf{h}_\theta(x), \mathbf{r}_k)}}{\sum_{k'=1}^K e^{-\epsilon_1 \alpha f(\mathbf{h}_\theta(x), \mathbf{r}_{k'})}} \quad (4)$$

with  $\alpha \in [0, +\infty)$ . The function  $G_{k,f}$  defined by Eq. 4 is differentiable wrt  $\theta, \mathcal{R}$  and  $\alpha$  (condition (i)) as it is a composition of functions differentiable wrt these variables. Furthermore, one has:

**Property 3.2** *(condition (ii)) If  $c_f(\mathbf{h}_\theta(x); \mathcal{R})$  is unique for all  $x \in \mathcal{X}$ , then:*

$$\lim_{\alpha \rightarrow +\infty} G_{k,f}(\mathbf{h}_\theta(x), \alpha; \mathcal{R}) = \begin{cases} 1 & \text{if } \mathbf{r}_k = c_f(\mathbf{h}_\theta(x); \mathcal{R}) \\ 0 & \text{otherwise} \end{cases}$$

**Proof:** Let  $\mathbf{r}_j = c_f(\mathbf{h}_\theta(x); \mathcal{R})$  and let us assume that  $f$  is a distance. One has:

$$\sum_{k'=1}^K e^{-\alpha f(\mathbf{h}_\theta(x), \mathbf{r}_{k'})} = e^{-\alpha f(\mathbf{h}_\theta(x), \mathbf{r}_j)} \times \left( 1 + \sum_{k' \neq j} e^{-\alpha (f(\mathbf{h}_\theta(x), \mathbf{r}_{k'}) - f(\mathbf{h}_\theta(x), \mathbf{r}_j))} \right)$$

As  $f(\mathbf{h}_\theta(x), \mathbf{r}_j) < f(\mathbf{h}_\theta(x), \mathbf{r}_{k'}), \forall k' \neq j$ , one has:

$$\lim_{\alpha \rightarrow +\infty} e^{-\alpha (f(\mathbf{h}_\theta(x), \mathbf{r}_{k'}) - f(\mathbf{h}_\theta(x), \mathbf{r}_j))} = 0$$

Thus  $\lim_{\alpha \rightarrow +\infty} G_{k,f}(\mathbf{h}_\theta(x), \alpha; \mathcal{R}) = 0$  if  $k \neq j$  and 1 if  $k = j$ . The case where  $f$  is a similarity function can be treated in the same way.  $\square$

The assumption that  $c_f(\mathbf{h}_\theta(x); \mathcal{R})$  is unique for all objects is necessary for  $G_{k,f}$  to take on binary values in the limit; it is not necessary to hold for small values of  $\alpha$ . In the unlikely event that the above assumption does not hold for some  $x$  and large  $\alpha$ , one can slightly perturbate the representatives equidistant to  $x$  prior to update them. We have never encountered this situation in practice.

Finally, Eq. 4 defines a valid (according to conditions (i) and (ii)) function  $G_{k,f}$  that can be used to solve the deep  $k$ -Means problem (2). We adopt this function in the remainder of this study.

Prior to studying the effect of  $\alpha$  in Eq. 4, we want to mention another possible choice for  $G_{k,f}$ . As  $G_{k,f}(\mathbf{h}_\theta(x), \alpha; \mathcal{R})$  plays the role of a closeness function for object  $x$  wrt representative  $\mathbf{r}_k$ , membership functions used in fuzzy clustering are potential candidates for  $G_{k,f}$ . In particular, the membership function of the fuzzy  $C$ -Means algorithm [4] is a valid candidate according to conditions (i) and (ii). It takes the form, for distance functions:

$$G_{k,f}(\mathbf{h}_\theta(x), \alpha; \mathcal{R}) = \left( \sum_{k'=1}^K \left( \frac{f(\mathbf{h}_\theta(x), \mathbf{r}_k)}{f(\mathbf{h}_\theta(x), \mathbf{r}_{k'})} \right)^{\frac{2}{\alpha-1}} \right)^{-1}$$

with  $\alpha$  defined on  $(1; +\infty)$  and  $\alpha_0$  (condition (ii)) equal to 1. However, in addition to being slightly more complex than the parametrized softmax, this formulation presents the disadvantage that it may be undefined when a representative coincides with an object; another assumption (in addition to the uniqueness assumption) is required here to avoid such a case.

### 3.2 Choice of $\alpha$

The parameter  $\alpha$  can be defined in different ways. Indeed,  $\alpha$  can play the role of an inverse temperature such that, when  $\alpha$  is 0, each data point in the embedding space is equally close, through  $G_{k,f}$ , to all the representatives (corresponding to a completely soft assignment), whereas when  $\alpha$  is  $+\infty$ , the assignment is hard. In the first case, for the deep  $k$ -Means optimization problem, all representatives are equal and set to the point  $\mathbf{r} \in \mathbb{R}^p$  that minimizes  $\sum_{x \in \mathcal{X}} \epsilon_1 f(\mathbf{h}_\theta(x), \mathbf{r})$ . In the second case, the solution corresponds to exactly performing  $k$ -Means in the embedding space, the latter being learned jointly with the clustering process. Following a deterministic annealing approach [26], one can start with a low value of  $\alpha$  (close to 0), and gradually increase it till a sufficiently large value is obtained. At first, representatives are randomly initialized. As the problem is smooth when  $\alpha$  is close to 0, different initializations are likely to lead to the same local minimum in the first iteration; this local minimum is used for the new values of the representatives for the second iteration, and so on. The continuity of  $G_{k,f}$  wrt  $\alpha$  implies that, provided the increment in  $\alpha$  is not too important, one evolves smoothly from the initial local minimum to the last one.

In the above deterministic annealing scheme,  $\alpha$  allows one to initialize cluster representatives. The initialization of the auto-encoder can as well have an important impact on the results obtained and prior studies (*e.g.*, [15, 29, 11, 30]) have relied on pretraining for this matter. In such a case, one can choose a high value for  $\alpha$  to directly obtain the behavior of the  $k$ -Means algorithm in the embedding space after pretraining. We evaluate both approaches in our experiments (Section 4).

Algorithm 1 summarizes the deep  $k$ -Means algorithm for the deterministic annealing scheme, where  $m_\alpha$  (respectively  $M_\alpha$ ) denote the minimum (respectively maximum) value of  $\alpha$ , and  $T$  is the number of epochs per each value of  $\alpha$  for the stochastic gradient updates. Even though  $M_\alpha$  is finite, it can be set sufficiently large to obtain in practice a hard assignment to representatives. Alternatively, when using pretraining, one sets  $m_\alpha = M_\alpha$  (*i.e.*, a constant  $\alpha$  is used).

## 4 Experiments

In order to evaluate the clustering results of our approach, we conducted experiments on different datasets and compared it against state-of-the-art standard and  $k$ -Means-related deep clustering models.

---

**Algorithm 1:** Deep  $k$ -Means algorithm

---

**Input:** data  $\mathcal{X}$ , number of clusters  $K$ , balancing parameter  $\lambda$ , scheme for  $\alpha$ , number of epochs  $T$ , number of minibatches  $N$ , learning rate  $\eta$   
**Output:** autoencoder parameters  $\theta$ , cluster representatives  $\mathcal{R}$   
Initialize  $\theta$  and  $\mathbf{r}_k$ ,  $1 \leq k \leq K$  (randomly or through pretraining)  
**for**  $\alpha = m_\alpha$  **to**  $M_\alpha$  **do** # inverse temperature levels  
    **for**  $t = 1$  **to**  $T$  **do** # epochs per  $\alpha$   
        **for**  $n = 1$  **to**  $N$  **do** # minibatches  
            Draw a minibatch  $\tilde{\mathcal{X}} \subset \mathcal{X}$   
            Update  $(\theta, \mathcal{R})$  using SGD (Eq. 3)  
        **end**  
    **end**  
**end**

---

#### 4.1 Datasets

The datasets used in the experiments are standard clustering benchmark collections. We considered both image and text datasets to demonstrate the general applicability of our approach. Image datasets consist of **MNIST** (70,000 images,  $28 \times 28$  pixels, 10 classes) and **USPS** (9,298 images,  $16 \times 16$  pixels, 10 classes) which both contain hand-written digit images. We reshaped the images to one-dimensional vectors and normalized the pixel intensity levels (between 0 and 1 for MNIST, and between -1 and 1 for USPS). The text collections we considered are the 20 Newsgroups dataset (hereafter, **20NEWS**) and the RCV1-v2 dataset (hereafter, **RCV1**). For 20NEWS, we used the whole dataset comprising 18,846 documents labeled into 20 different classes. Similarly to [29, 11], we sampled from the full RCV1-v2 collection a random subset of 10,000 documents, each of which pertains to only one of the four largest classes. Because of the text datasets' sparsity, and as proposed in [29], we selected the 2000 words with the highest tf-idf values to represent each document.

#### 4.2 Baselines and Deep $k$ -Means variants

Clustering models may use different strategies and different clustering losses, leading to different properties. As our goal in this work is to study the  $k$ -Means clustering algorithm in embedding spaces, we focus on the family of  $k$ -Means-related models and compare our approach against state-of-the-art models from this family, using both standard and deep clustering models. For the standard clustering methods, we used: the  $k$ -Means clustering approach [21] with initial cluster center selection [2], denoted **KM**; an approach denoted as **AE-KM** in which dimensionality reduction is first performed using an auto-encoder followed by  $k$ -Means applied to the learned representations.

For the joint deep clustering models, the only previous, "true" deep clustering  $k$ -Means-related method is the Deep Clustering Network (DCN) approach described in [30]. In addition, we consider here the Improved Deep Embedded Clustering (IDEC) model [11] as an additional baseline. IDEC is, to the best of our knowledge, the state-of-the-art approach in the centroid-based – therefore related to  $k$ -Means – deep clustering family. IDEC is an improved version of the DEC model [29]. For both of these approaches, we studied two variants: with pretraining (**DCN<sup>p</sup>** and **IDEC<sup>p</sup>**) and without pretraining (**DCN<sup>np</sup>** and **IDEC<sup>np</sup>**). The pretraining we performed here simply consists in initializing the weights by training the auto-encoder on the data to minimize the reconstruction loss in an end-to-end fashion – we did not use layer-wise pretraining [3].

The proposed Deep  $k$ -Means (DKM) is, as DCN, a "true"  $k$ -Means approach in the embedding space; it jointly learns AE-based representations and relaxes the  $k$ -Means problem by introducing a parameterized softmax as a differentiable surrogate to  $k$ -Means argmin. In the experiments, we considered two variants of this approach. **DKM<sup>a</sup>** implements an annealing strategy for the inverse temperature  $\alpha$  and does not rely on pretraining. The scheme we used for the evolution of the inverse temperature  $\alpha$  in **DKM<sup>a</sup>** is given by the following recursive sequence:  $\alpha_{n+1} = 2^{1/\log(n)^2} \times \alpha_n$  with  $m_\alpha = \alpha_1 = 0.1$ . The 40 first terms of  $(\alpha_n)$  are plotted in Figure 2. The rationale behind the choice of this scheme is that we want  $\alpha$  to spend more iterations on smaller values and less on larger values while preserving a gentle slope. Alternatively, we studied the variant **DKM<sup>p</sup>** which is

initialized by pretraining an auto-encoder and then follows Algorithm 1 with a constant  $\alpha$  such that  $m_\alpha = M_\alpha = 1000$ . Such a high  $\alpha$  is equivalent to having hard cluster assignments while maintaining the differentiability of the optimization problem.

**Implementation details.** For IDEC, we used the Keras code shared by their authors.<sup>1</sup> Our own code for DKM is based on TensorFlow. To enable full control of the comparison between DCN and DKM – DCN being the closest competitor to DKM – we also re-implemented DCN in TensorFlow. The code for both DKM and DCN is available online.<sup>2</sup>

**Choice of  $f$  and  $g$ .** The functions  $f$  and  $g$  in Problem (1) define which similarity/distance function is used for the clustering loss and reconstruction error, respectively. In this study, both  $f$  and  $g$  are simply instantiated with the Euclidean distance on all datasets. For the sake of comprehensiveness, we report in the supplementary material results for the cosine distance on 20NEWS.

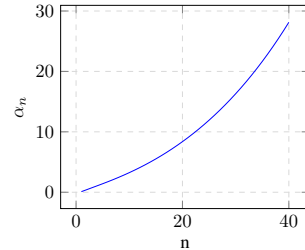


Figure 2: Annealing scheme for inverse temperature  $\alpha$ , following the sequence  $\alpha_{n+1} = 2^{1/\log(n)^2} \times \alpha_n$ ;  $\alpha_1 = 0.1$ .

### 4.3 Experimental setup

**Auto-encoder description and training details.** The auto-encoder we used in the experiments is the same across all datasets and is borrowed from previous deep clustering studies [29, 11]. Its encoder is a fully-connected multilayer perceptron with dimensions  $d$ -500-500-2000- $K$ , where  $d$  is the original data space dimension and  $K$  is the number of clusters to obtain. The decoder is a mirrored version of the encoder. All layers except the one preceding the embedding layer and the one preceding the output layer are applied a ReLU activation function [23] before being fed to the next layer. For the sake of simplicity, we did not rely on any complementary training or regularization strategies such as batch normalization or dropout. The auto-encoder weights are initialized following the Xavier scheme [10]. For all deep clustering approaches, the training is based on the Adam optimizer [19] with standard learning rate  $\eta = 0.001$  and momentum rates  $\beta_1 = 0.9$  and  $\beta_2 = 0.999$ . The minibatch size is set to 256 on all datasets following [11]. We emphasize that we chose exactly the same training configuration for all models to facilitate a fair comparison.

The number of pretraining epochs is set to 50 for all models relying on pretraining. The number of fine-tuning epochs for DCN<sup>p</sup> and IDEC<sup>p</sup> is fixed to 50 (or equivalently in terms of iterations: 50 times the number of minibatches). We set the number of training epochs for DCN<sup>np</sup> and IDEC<sup>np</sup> to 200. For DKM<sup>a</sup>, we used the 40 terms of the sequence  $\alpha$  given in Figure 2 as the annealing scheme and performed 5 epochs for each  $\alpha$  term (*i.e.*, 200 epochs in total). DKM<sup>p</sup> is fine-tuned by performing 100 epochs with constant  $\alpha = 1000$ . The cluster representatives are initialized randomly from a uniform distribution  $U(-1, 1)$  for models without pretraining. In case of pretraining, the cluster representatives are initialized by applying  $k$ -Means to the pretrained embedding space.

**Hyperparameter selection.** The hyperparameters  $\lambda$  for DCN and DKM and  $\gamma$  for IDEC, that define the trade-off between the reconstruction and the clustering error in the loss function, were determined by performing a line search on the set  $\{10^i \mid i \in [-4, 3]\}$ . To do so, we randomly split each dataset into a validation set (10% of the data) and a test set (90%). Each model is trained on the whole data and only the validation set labels are leveraged in the line search to identify the optimal  $\lambda$  or  $\gamma$  (optimality is measured with respect to the clustering accuracy metric). We provide the validation-optimal  $\lambda$  and  $\gamma$  obtained for each model and dataset in the supplementary material. The performance reported in the following sections corresponds to the evaluation performed only on the *held-out test set*.

While one might argue that such procedure affects the unsupervised nature of the clustering approaches, we believe that a clear and transparent hyperparameter selection methodology is preferable

<sup>1</sup><https://github.com/XifengGuo/IDEC-toy>. We used this version instead of <https://github.com/XifengGuo/IDEC> as only the former enables auto-encoder pretraining in a non-layer-wise fashion.

<sup>2</sup>[https://github.com/\\*\\*\\*/\\*\\*\\*](https://github.com/***/***) (anonymized)

Table 1: Clustering results of the compared methods. Performance is measured in terms of NMI and clustering accuracy (%); higher is better. Each cell contains the average and standard deviation computed over 10 runs. The best result for each dataset/metric is underlined. Bold values correspond to results with no significant difference ( $p > 0.05$ ) to the best.

| Model  | MNIST           |                 | USPS            |                 | 20NEWS          |                 | RCV1            |                 |
|--|-----------------|-----------------|-----------------|-----------------|-----------------|-----------------|-----------------|-----------------|
|  | ACC             | NMI             | ACC             | NMI             | ACC             | NMI             | ACC             | NMI             |
| KM   | 53.5±0.3        | 49.8±0.5        | 67.3±0.1        | 61.4±0.1        | 23.2±1.5        | 21.6±1.8        | 50.8±2.9        | <b>31.3±5.4</b> |
| AE-KM  | 80.8±1.8        | 75.2±1.1        | 72.9±0.8        | 71.7±1.2        | <b>49.0±2.9</b> | 44.5±1.5        | <b>56.7±3.6</b> | <b>31.5±4.3</b> |
| Deep clustering approaches without pretraining |                 |                 |                 |                 |                 |                 |                 |                 |
| DCN <sup>np</sup>                              | 34.8±3.0        | 18.1±1.0        | 36.4±3.5        | 16.9±1.3        | 17.9±1.0        | 9.8±0.5         | 41.3±4.0        | 6.9±1.8         |
| IDEC <sup>np</sup>                             | 61.8±3.0        | 62.4±1.6        | 53.9±5.1        | 50.0±3.8        | 22.3±1.5        | 22.3±1.5        | <b>56.7±5.3</b> | <b>31.4±2.8</b> |
| DKM <sup>a</sup>                               | 82.3±3.2        | 78.0±1.9        | <b>75.5±6.8</b> | 73.0±2.3        | 44.8±2.4        | 42.8±1.1        | <b>53.8±5.5</b> | 28.0±5.8        |
| Deep clustering approaches with pretraining    |                 |                 |                 |                 |                 |                 |                 |                 |
| DCN <sup>p</sup>                               | 81.1±1.9        | 75.7±1.1        | 73.0±0.8        | 71.9±1.2        | <b>49.2±2.9</b> | 44.7±1.5        | <b>56.7±3.6</b> | <b>31.6±4.3</b> |
| IDEC <sup>p</sup>                              | <b>85.7±2.4</b> | <b>86.4±1.0</b> | <b>75.2±0.5</b> | 74.9±0.6        | 40.5±1.3        | 38.2±1.0        | <b>59.5±5.7</b> | <b>34.7±5.0</b> |
| DKM <sup>p</sup>                               | <b>84.0±2.2</b> | 79.6±0.9        | <b>75.7±1.3</b> | <b>77.6±1.1</b> | <b>51.2±2.8</b> | <b>46.7±1.2</b> | <b>58.3±3.8</b> | <b>33.1±4.9</b> |

to a vague or hidden one. Moreover, although we did not explore such possibility in this study, it might be possible to define this trade-off hyperparameter in a data-driven way.

**Experimental protocol.** We observed in pilot experiments that the clustering performance of the different models is subject to non-negligible variance from one run to another. This variance is due to the randomness in the initialization and in the minibatch sampling for the stochastic optimizer. When pretraining is used, the variance of the general pretraining phase and that of the model-specific fine-tuning phase add up, which makes it difficult to draw any confident conclusion about the clustering ability of a model. To alleviate this issue, we compared the different approaches using seeded runs whenever this was possible. This has the advantage of removing the variance of pretraining as seeds guarantee exactly the same results at the end of pretraining (since the same pretraining is performed for the different models). Additionally, it ensures that the same sequence of minibatches will be sampled. In practice, we used seeds for the models implemented in TensorFlow (KM, AE-KM, DCN and DKM). Because of implementation differences, seeds could not give the same pretraining states in the Keras-based IDEC. All in all, we randomly selected 10 seeds and for each model performed one run per seed. Additionally, to account for the remaining variance and to report statistical significance, we performed a Student’s  $t$ -test from the 10 collected samples (i.e., runs).

#### 4.4 Clustering results

The results for the evaluation of the compared clustering methods on the different benchmark datasets are summarized in Table 1. The clustering performance is evaluated with respect to two standard measures [6]: Normalized Mutual Information (NMI) and the clustering accuracy (ACC). We report for each dataset/method pair the average and standard deviation of these metrics computed over 10 runs and conduct significance testing as described in Section 4.3. The underlined result in each column of Table 1 corresponds to the best result for the corresponding dataset/metric. Results in bold can be considered as equivalent to the best as their difference thereto is not statistically significant ( $p > 0.05$ ).

We first observe that when no pretraining is used, DKM with annealing (DKM<sup>a</sup>) markedly outperforms other deep clustering approaches (DCN<sup>np</sup> and IDEC<sup>np</sup>) on all datasets except RCV1. DKM<sup>a</sup> achieves clustering performance similar to that obtained by pretraining-based methods. This confirms our intuition that the proposed annealing strategy can be seen as an alternative to pretraining.

Among the approaches integrating representation learning with pretraining, the AE-KM method, that separately performs dimension reduction and  $k$ -Means clustering, overall obtains the worst results. This observation is in line with prior studies [30, 11] and underlines again the importance of jointly learning representations and clustering. We note as well that, apart from DKM<sup>a</sup>, all pretraining-based deep clustering approaches substantially outperform their non-pretrained counterparts, which stresses the importance of pretraining.

Table 2: Clustering results for  $k$ -Means applied to different learned embedding spaces to measure the  $k$ -Means-friendliness of each method. Performance is measured in terms of NMI and clustering accuracy (%); higher is better. Each cell contains the average and standard deviation computed over 10 runs. The best result for each dataset/metric is underlined. Bold values correspond to results with no significant difference ( $p > 0.05$ ) to the best.

| Model                 | MNIST           |                 | USPS            |                 | 20NEWS          |                 | RCV1            |                 |
|-----------------------|-----------------|-----------------|-----------------|-----------------|-----------------|-----------------|-----------------|-----------------|
|                       | ACC             | NMI             | ACC             | NMI             | ACC             | NMI             | ACC             | NMI             |
| AE-KM                 | 80.8±1.8        | 75.2±1.1        | 72.9±0.8        | 71.7±1.2        | 49.0±2.9        | 44.5±1.5        | <b>56.7±3.6</b> | <b>31.5±4.3</b> |
| DCN <sup>P</sup> + KM | <b>84.9±3.1</b> | <b>79.4±1.5</b> | <b>73.9±0.7</b> | 74.1±1.1        | <b>50.5±3.1</b> | <b>46.5±1.6</b> | <b>57.3±3.6</b> | <b>32.3±4.4</b> |
| DKM <sup>a</sup> + KM | <b>84.8±1.3</b> | <b>78.7±0.8</b> | <b>76.9±4.9</b> | 74.3±1.5        | 49.0±2.5        | 44.0±1.0        | <b>53.4±5.9</b> | 27.4±5.3        |
| DKM <sup>P</sup> + KM | <b>85.1±3.0</b> | <b>79.9±1.5</b> | <b>75.7±1.3</b> | <b>77.6±1.1</b> | <b>52.1±2.7</b> | <b>47.1±1.3</b> | <b>58.3±3.8</b> | <b>33.0±4.9</b> |

Furthermore, DKM<sup>P</sup> yields significant improvements on all collections except RCV1 over DCN<sup>P</sup>, the other “true” deep  $k$ -Means approach. In all cases, DCN<sup>P</sup> shows performance on par with that of AE-KM. This places, to the best of our knowledge, DKM<sup>P</sup> as the current best deep  $k$ -Means clustering method. IDECP also outperforms DCN<sup>P</sup> on all datasets except 20NEWS on which its results are considerably lower. IDECP sometimes reports performance which is similar or better – albeit mostly statistically insignificant – to DKM<sup>P</sup>’s, however optimizing a different loss. All in all, accounting for the different metrics and datasets as well as statistical significance, DKM<sup>P</sup> can be considered as the most consistently effective among centroid-based deep clustering approaches.

#### 4.5 $k$ -Means-friendliness of the learned representations

In the previous experiment, we investigated the clustering ability of the different models. While the quality of the clustering results and that of the representations learned by the models are likely to be correlated, it is relevant to study to what extent learned representations are distorted to facilitate clustering – in other words, how they are biased towards “clustering-friendliness”. More specifically, we focus on the representations learned by the deep clustering approaches related to  $k$ -Means: DCN<sup>P</sup>, DKM<sup>a</sup>, and DKM<sup>P</sup> (DCN<sup>np</sup> was discarded due to its poor clustering performance). We analyze how effective applying  $k$ -Means to these representations is in comparison to applying  $k$ -Means to the AE-learned representations (*i.e.*, AE-KM).

The results of this experiment are reported in Table 2. We can observe that on most datasets the representations learned by  $k$ -Means-related deep clustering approaches lead to significant improvement wrt AE-learned representations. This confirms that all these deep clustering methods truly bias their representations. Interestingly, we note that applying  $k$ -Means to the representations learned by DCN<sup>P</sup> yields substantial improvements in comparison to the results reported in Table 1. Overall, although the difference is not statistically significant on all datasets/metrics, the representations learned by DKM<sup>P</sup> are shown to be the most appropriate to  $k$ -Means. This goes in line with the insight gathered from Section 4.4.

To further support this latter finding and to bring a more interpretable view of the learned representations, we illustrate the embedded samples provided by AE, DCN<sup>P</sup>, DKM<sup>a</sup>, DKM<sup>P</sup> on USPS in Figure 3 (best viewed in color). We used for that matter the  $t$ -SNE visualization method [27] which projected embeddings into a 2D space. We observe that the representations for points from different clusters are clearly better separated and disentangled in DKM<sup>P</sup> than in other models. This once again supports the superior ability of DKM<sup>P</sup> to learn  $k$ -Means-friendly representations.

## 5 Conclusion

We have presented in this paper a new approach for jointly clustering with  $k$ -Means and learning representations by considering the  $k$ -Means clustering loss as the limit of a differentiable function. To the best of our knowledge, this is the first approach that truly jointly optimizes, through simple stochastic gradient descent updates, representation and  $k$ -Means clustering losses. In addition to pretraining, that can be used in all methods, this approach can also rely on a deterministic annealing scheme for parameter initialization.

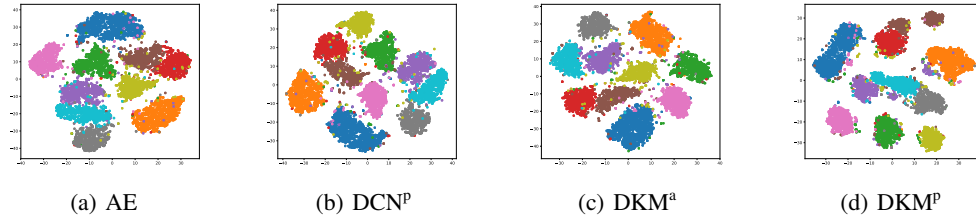


Figure 3: t-SNE visualization of the embedding spaces learned on USPS.

We further conducted careful comparisons with previous approaches by ensuring that the same architecture, initialization and sequence minibatches are used. The experiments conducted on several datasets confirm the good behavior of the proposed approach that outperforms DCN, the current best approach for  $k$ -Means clustering in embedding spaces, on all the collections considered.

## References

- [1] E. Aljalbout, V. Golkov, Y. Siddiqui, and D. Cremers. Clustering with Deep Learning: Taxonomy and New Methods. *arXiv:1801.07648*, 2018.
- [2] D. Arthur and S. Vassilvitskii. K-Means++: the Advantages of Careful Seeding. In *Proceedings of the 18th Annual ACM-SIAM Symposium on Discrete algorithms*, SODA ’07, pages 1027–1025, 2007.
- [3] Y. Bengio, P. Lamblin, D. Popovici, and H. Larochelle. Greedy Layer-Wise Training of Deep Networks. In *Proceedings of the 20th Annual Conference on Neural Information Processing Systems*, NIPS ’06, pages 153–160, 2006.
- [4] J. C. Bezdek, R. Ehrlich, and W. Full. FCM: The Fuzzy c-Means Clustering Algorithm. *Computers & Geosciences*, 10(2-3):191–203, 1984.
- [5] C. M. Bishop. *Pattern Recognition and Machine Learning*. Springer, 2006.
- [6] D. Cai, X. He, and J. Han. Locally Consistent Concept Factorization for Document Clustering. *IEEE Transactions on Knowledge and Data Engineering*, 23(6):902–913, 2011.
- [7] J. Chang, L. Wang, G. Meng, S. Xiang, and C. Pan. Deep Adaptive Image Clustering. In *Proceedings of the 2017 IEEE International Conference on Computer Vision*, ICCV ’17, pages 5879–5887, 2017.
- [8] N. Dilokthanakul, P. A. M. Mediano, M. Garnelo, M. C. H. Lee, H. Salimbeni, K. Arulkumaran, and M. Shanahan. Deep Unsupervised Clustering with Gaussian Mixture Variational Autoencoders. *arXiv:1611.02648*, 2017.
- [9] K. G. Dizaji, A. Herandi, C. Deng, W. Cai, and H. Huang. Deep Clustering via Joint Convolutional Autoencoder Embedding and Relative Entropy Minimization. In *Proceedings of the 2017 IEEE International Conference on Computer Vision*, ICCV ’17, pages 5736–5745, 2017.
- [10] X. Glorot and Y. Bengio. Understanding the Difficulty of Training Deep Feedforward Neural Networks. In *Proceedings of the 13th International Conference on Artificial Intelligence and Statistics*, AISTATS ’10, pages 249–256, 2010.
- [11] X. Guo, L. Gao, X. Liu, and J. Yin. Improved Deep Embedded Clustering with Local Structure Preservation. In *Proceedings of the 26th International Joint Conference on Artificial Intelligence*, IJCAI ’17, pages 1753–1759, 2017.
- [12] G. E. Hinton and R. R. Salakhutdinov. Reducing the Dimensionality of Data with Neural Networks. *Science*, 313(5786):504–507, 2006.
- [13] C.-C. Hsu and C.-W. Lin. CNN-Based Joint Clustering and Representation Learning with Feature Drift Compensation for Large-Scale Image Data. *IEEE Transactions on Multimedia*, 20(2):421–429, 2018.
- [14] W. Hu, T. Miyato, S. Tokui, E. Matsumoto, and M. Sugiyama. Learning Discrete Representations via Information Maximizing Self-Augmented Training. In *Proceedings of the 34th International Conference on Machine Learning*, ICML ’17, pages 1558–1567, 2017.
- [15] P. Huang, Y. Huang, W. Wang, and L. Wang. Deep Embedding Network for Clustering. In *Proceedings of the 22nd International Conference on Pattern Recognition*, ICPR ’14, pages 1532–1537, 2014.
- [16] E. Jang, S. Gu, and B. Poole. Categorical Reparameterization with Gumbel-Softmax. In *Proceedings of the 5th International Conference on Learning Representations*, ICLR ’17, 2017.

- [17] P. Ji, T. Zhang, H. Li, M. Salzmann, and I. Reid. Deep Subspace Clustering Networks. In *Proceedings of the 31st Annual Conference on Neural Information Processing Systems, NIPS '17*, pages 23–32, 2017.
- [18] Z. Jiang, Y. Zheng, H. Tan, B. Tang, and H. Zhou. Variational Deep Embedding: An Unsupervised and Generative Approach to Clustering. In *Proceedings of the 26th International Joint Conference on Artificial Intelligence, IJCAI '17*, pages 1965–1972, 2017.
- [19] D. P. Kingma and J. L. Ba. Adam: a Method for Stochastic Optimization. In *Proceedings of the 3rd International Conference on Learning Representations, ICLR '15*, 2015.
- [20] H. W. Kuhn. The Hungarian Method for the Assignment Problem. *Naval Research Logistics Quarterly*, 2(1-2):83–97, 1955.
- [21] J. MacQueen. Some Methods for Classification and Analysis of Multivariate Observations. In *Proceedings of the 5th Berkeley Symposium on Mathematical Statistics and Probability*, pages 281–297, 1967.
- [22] C. J. Maddison, A. Mnih, and Y. W. Teh. The Concrete Distribution: A Continuous Relaxation of Discrete Random Variables. In *Proceedings of the 5th International Conference on Learning Representations, ICLR '17*, 2017.
- [23] V. Nair and G. E. Hinton. Rectified Linear Units Improve Restricted Boltzmann Machines. In *Proceedings of the 27th International Conference on Machine Learning, ICML '10*, pages 807–814, 2010.
- [24] X. Peng, J. Feng, J. Lu, W.-y. Yau, and Z. Yi. Cascade Subspace Clustering. In *Proceedings of the 31th Conference on Artificial Intelligence, AAAI '17*, pages 2478–2484, 2017.
- [25] X. Peng, S. Xiao, J. Feng, W. Y. Yau, and Z. Yi. Deep Subspace Clustering with Sparsity Prior. In *Proceedings of the 25th International Joint Conference on Artificial Intelligence, IJCAI '16*, pages 1925–1931, 2016.
- [26] K. Rose, E. Gurewitz, and G. Fox. A Deterministic Annealing Approach to Clustering. *Pattern Recognition Letters*, 11(9):589–594, 1990.
- [27] L. van der Maaten and G. Hinton. Visualizing Data using t-SNE. *Journal of Machine Learning Research*, 9:2579–2605, 2008.
- [28] N. X. Vinh, J. Epps, and J. Bailey. Information Theoretic Measures for Clusterings Comparison: Variants, Properties, Normalization and Correction for Chance. *Journal of Machine Learning Research*, 11:2837–2854, 2010.
- [29] J. Xie, R. Girshick, and A. Farhadi. Unsupervised Deep Embedding for Clustering Analysis. In *Proceedings of the 33rd International Conference on Machine Learning, ICML '16*, pages 478–487, 2016.
- [30] B. Yang, X. Fu, N. D. Sidiropoulos, and M. Hong. Towards K-means-friendly Spaces: Simultaneous Deep Learning and Clustering. In *Proceedings of the 34th International Conference on Machine Learning, ICML '17*, pages 3861–3870, 2017.
- [31] J. Yang, D. Parikh, and D. Batra. Joint Unsupervised Learning of Deep Representations and Image Clusters. In *Proceedings of the 2016 IEEE Conference on Computer Vision and Pattern Recognition, CVPR '16*, pages 5147–5156, 2016.

## A Evaluation measures

In our experiments, the clustering performance of the evaluated methods is evaluated with respect to two standard measures [6]: Normalized Mutual Information (NMI) and the clustering accuracy (ACC). NMI is an information-theoretic measure based on the mutual information of the ground-truth classes and the obtained clusters, normalized using the entropy of each. Formally, let  $S = \{S_1, \dots, S_K\}$  and  $C = \{C_1, \dots, C_K\}$  denote the ground-truth classes and the obtained clusters, respectively.  $S_i$  (resp.  $C_j$ ) is the subset of data points from class  $i$  (resp. cluster  $j$ ). Let  $N$  be the number of points in the dataset. The NMI is computed according to the following formula:

$$\text{NMI}(C, S) = \frac{I(C, S)}{\sqrt{H(C) \times H(S)}}$$

where  $I(C, S) = \sum_{i,j} \frac{|C_i \cap S_j|}{N} \log \frac{N|C_i \cap S_j|}{|C_i||S_j|}$  corresponds to the mutual information between the partitions  $C$  and  $S$ , and  $H(C) = -\sum_i \frac{|C_i|}{N} \log \frac{|C_i|}{N}$  is the entropy of  $C$ .

On the other hand, ACC measures the proportion of data points for which the obtained clusters can be correctly mapped to ground-truth classes, where the matching is based on the Hungarian algorithm [20]. Let  $s_i$  and  $c_i$  further denote the ground-truth class and the obtained cluster, respectively, to which data point  $x_i$ ,  $i \in \{1, \dots, N\}$  is assigned. Then the clustering accuracy is defined as follows:

$$\text{ACC}(C, S) = \max_{\phi} \frac{1}{N} \sum_{i=1}^N \mathbb{I}\{s_i = \phi(c_i)\}$$

Table 3: Statistics of the datasets and dataset-specific optimal trade-off hyperparameters ( $\lambda$  for DKM-based and DCN-based methods and  $\gamma$  for IDEC-based ones) determined on the validation set.

| Dataset                            | MNIST          | USPS           | 20NEWS    | RCV1      |
|------------------------------------|----------------|----------------|-----------|-----------|
| #Samples                           | 70,000         | 9,298          | 18,846    | 10,000    |
| #Classes                           | 10             | 10             | 20        | 4         |
| Dimensions                         | $28 \times 28$ | $16 \times 16$ | 2,000     | 2,000     |
| $\lambda_{\text{DKM}}^a$           | $10^{-1}$      | $10^{-1}$      | $10^{-4}$ | $10^{-4}$ |
| $\lambda_{\text{DKM}}^p$           | 1              | 1              | $10^{-1}$ | $10^{-2}$ |
| $\lambda_{\text{DCN}}^p$           | 10             | $10^{-1}$      | $10^{-1}$ | $10^{-1}$ |
| $\lambda_{\text{DCN}}^{\text{np}}$ | $10^{-2}$      | $10^{-1}$      | $10^{-4}$ | $10^{-3}$ |
| $\gamma_{\text{IDEC}}^p$           | $10^{-2}$      | $10^3$         | $10^{-1}$ | $10^{-3}$ |
| $\gamma_{\text{IDEC}}^{\text{np}}$ | $10^{-3}$      | $10^{-1}$      | $10^{-3}$ | $10^{-4}$ |

where  $\mathbb{I}$  denotes the indicator function:  $\mathbb{I}\{\text{true}\} = 1$  and  $\mathbb{I}\{\text{false}\} = 0$ ;  $\phi$  is a mapping from cluster labels to class labels.

We additionally report in this supplementary material the clustering performance wrt to the adjusted Rand index (ARI) [28]. ARI counts the pairs of data points on which the classes and clusters agree or disagree, and is corrected for chance. Formally, ARI is given by:

$$\text{ARI}(C, S) = \frac{\sum_{ij} \binom{|C_i \cap S_j|}{2} - \binom{N}{2}^{-1} \sum_i \binom{|C_i|}{2} \sum_j \binom{|S_j|}{2}}{\frac{1}{2} \left( \sum_i \binom{|C_i|}{2} + \sum_j \binom{|S_j|}{2} \right) - \binom{N}{2}^{-1} \sum_i \binom{|C_i|}{2} \sum_j \binom{|S_j|}{2}}$$

## B Dataset statistics and optimal hyperparameters

We summarize in Table 3 the statistics of the different datasets used in the experiments, as well as the dataset-specific optimal values of the hyperparameter ( $\lambda$  for DKM-based and DCN-based methods and  $\gamma$  for IDEC-based ones) which trades off between the reconstruction loss and the clustering loss. We remind that this optimal value was determined using a validation set, disjoint from the test set on which we reported results in the paper.

## C Additional results

The additional results given in this section have also been computed from 10 seeded runs whenever possible and Student’s  $t$ -test was performed from those 10 samples.

### C.1 ARI results

We report in Table 4 the results obtained by all approaches wrt the ARI measure on the datasets used in the paper.

### C.2 Cosine distance

The proposed Deep  $k$ -Means framework enables the use of different distance and similarity functions to compute the AE’s reconstruction error (based on function  $g$ ) and the clustering loss (based on function  $f$ ). In the paper, we adopted the euclidean distance for both  $f$  and  $g$ . For the sake of comprehensiveness, we performed additional experiments on DKM using different such functions. In particular, we showcase in Table 5 the results obtained by choosing the cosine distance for  $f$  and the euclidean distance for  $g$  ( $\text{DKM}_{\text{ce}}^a$  and  $\text{DKM}_{\text{ce}}^p$ ) in comparison to using euclidean distance for both  $f$  and  $g$  ( $\text{DKM}_{\text{ce}}^a$  and  $\text{DKM}_{\text{ce}}^p$ ) – these latter corresponding to the approaches reported in the paper. Note that for  $\text{DKM}_{\text{ce}}^a$  and  $\text{DKM}_{\text{ce}}^p$  as well the reported results correspond to those obtained with the optimal lambda determined on the validation set.

Table 4: Clustering results of the compared methods. Performance is measured in terms of ARI (%); higher is better. Each cell contains the average and standard deviation computed over 10 runs. The best result for each dataset/metric is underlined. Bold values correspond to results with no significant difference ( $p > 0.05$ ) to the best.

| Model  | MNIST           | USPS            | 20NEWS          | RCV1            |
|--|-----------------|-----------------|-----------------|-----------------|
| KM   | 36.6±0.1        | 53.5±0.1        | 7.6±0.9         | 20.6±2.8        |
| AE-KM  | 69.4±1.8        | 63.2±1.5        | 31.0±1.6        | 23.9±4.3        |
| Deep clustering approaches without pretraining |                 |                 |                 |                 |
| DCN <sup>np</sup>                              | 15.6±1.1        | 14.7±1.8        | 5.7±0.5         | 6.9±2.1         |
| IDEC <sup>np</sup>                             | 49.1±3.0        | 40.2±5.1        | 9.8±1.5         | <b>28.5±5.3</b> |
| DKM <sup>a</sup>                               | 73.6±3.1        | <b>66.3±4.9</b> | 26.7±1.5        | 20.7±4.4        |
| Deep clustering approaches with pretraining    |                 |                 |                 |                 |
| DCN <sup>p</sup>                               | 70.2±1.8        | 63.4±1.5        | 31.3±1.6        | 24.0±4.3        |
| IDEC <sup>p</sup>                              | <b>81.5±2.4</b> | <b>68.1±0.5</b> | 26.0±1.3        | <b>32.9±5.7</b> |
| DKM <sup>p</sup>                               | 75.0±1.8        | <b>68.5±1.8</b> | <b>33.9±1.5</b> | 26.5±4.9        |

Table 5: Clustering results for DKM using the euclidean and cosine distances on 20NEWS. Each cell contains the average and standard deviation computed over 10 runs. The best result for each dataset/metric is underlined. Bold values correspond to results with no significant difference ( $p > 0.05$ ) to the best.

| Model  | ACC             | NMI             | ARI             |
|--|-----------------|-----------------|-----------------|
| $f = \text{euclidean distance}, g = \text{euclidean distance}$ |                 |                 |                 |
| DKM <sub>ee</sub> <sup>a</sup>                                 | 44.8±2.4        | 42.8±1.1        | 26.7±1.5        |
| DKM <sub>ee</sub> <sup>p</sup>                                 | <b>51.2±2.8</b> | <b>46.7±1.2</b> | <b>33.9±1.5</b> |
| $f = \text{cosine distance}, g = \text{euclidean distance}$    |                 |                 |                 |
| DKM <sub>ce</sub> <sup>a</sup>                                 | <b>51.3±1.5</b> | 44.4±0.7        | 32.6±1.0        |
| DKM <sub>ce</sub> <sup>p</sup>                                 | <b>51.0±2.6</b> | 45.1±1.2        | <b>33.0±1.1</b> |